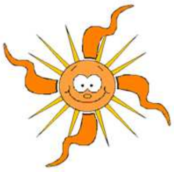

15th RHESSI Workshop, 26-30 July 2016,
Graz, Austria

Directivity and Polarization Dynamics of Hard X-Ray and Gamma-Ray Emission from Flare Loop

Melnikov V.F.[1], *Charikov Yu.E.* [2], *Kudriavtsev I.V.* [1,2]
([1]Pulkovo Observatory, [2]Ioffe Institute,
Saint Petersburg)

Particle Acceleration Processes

There exists a wide variety of acceleration mechanisms:

(1) electric DC-field acceleration (*current sheets, twisted loops*)

(2) shock acceleration (propagating MHD shocks; standing MHD shocks in reconnection outflows)

(3) betatron and first order Fermi acceleration (in collapsing magnetic traps);

(4) stochastic acceleration (*wave turbulence, microflares*)

2

Are there any constraints from observations?

The properties of the acceleration mechanisms are not the same. They may act in different places inside a flaring loop, and they may produce electrons with different types of pitch-angle distribution, Possibly, all of them can operate in solar flares!

Only observations can tell us which mechanism is dominant in a specific flare configuration.

The purpose of this talk is to show that spatially resolved observations can provide us with data about the **pitch-angle anisotropy of accelerated electrons** and, therefore, give us valuable constraints on acceleration models.

3

Pitch-angle distribution of accelerated electrons in flaring loops

The knowledge about the type of the pitch-angle distribution of accelerated electrons is crucial for selecting a correct mechanism or model of the electron acceleration in a specific solar flare.

Recently, we have got an ample evidence of existing different types of pitch-angle distributions of mildli relativistic electrons in flaring loops using spatially resolved observations in the microwave band (NoRH, 17 and 34 GHz):

- Isotropic and pancake-like anisotropy (Melnikov et al. ApJL 2002);

- Beam-like anisotropy (Altyntsev et al. ApJ 2008; Reznikova et al. ApJ 2009).

This discoveries become possible due to a very strong dependence of the gyrosynchrotron microwave emission on the parameters of the pitch-angle distribution of emitting mildly relativistic electrons (Fleishman & Melnikov ApJ 2003).

Note, however, that these new results relate only to electrons with relativistic energies (E ~> mc^2).

2016 4

Observation of HXR/Gamma-ray directivity

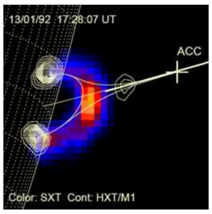

HXR and Gamma-ray observations can provide us with data on lower energy electrons.

One way to get information about the pith-angle distribution of electrons emitting HXR/gamma-ray emissions is to study their directivity.

So far, solar flare researchers did not succeed to make a definite conclusion on the directivity of HXR emission at photon energies 20-100 keV. The reason is the Compton backscattering of hard X-rays in the chromosphere which can completely mask the initial emission directivity.

The good candidates for the directivity search are behind the limb flares due to small scattering in the corona.
Another possibility is the observations at high photon energies where:
a) the directivity higher; b) Compton backscattering lower.

Statistical studies of the center-to-limb variation of the HXR/gamma-ray emission have definitely shown that:

1)the gamma emission (E~100-300 keV) is stronger on the solar limb;
2)Limb flares have harder energy spectrum than disk flares.
Bogovalov et al., *1985* (Venera-13), 37 flares in the range 50-300 кэВ;
Vestrand et al, 1987 (SMM/GRS), 72 events, 20-200 keV.

→ "Pancake" pitch-angle distribution near footpoints? - (Dermer and Ramaty, 1987)

2016 5

Space crafts for stereoscopic observations of HXR and Gamma-ray flare emissions

In the past, combined observations from spectrometers aboard:

ISEE-3 + PVO (Kane et al. 1988), 39 flares, E=100-1000 keV

Venera-13, 14 + SMM/GRS (Li et al. 1994), 28 flares, E=100-500 keV

Ulysses + Yohkoh (Kane et al. 1998), 8 flares, E=20-125 keV

In the current years, we have:

Near Mars orbit: HEND/MarsOdissey (2002 - now)
Near Earth orbits: RHESSI, Konus/Wind, INTEGRAL, GBM/Fermi

In the past, the stereoscopic observations of flares did not give definite statistical results on the directivity of HXR/gamma emissions: D~1. Although, there were some flares showing the directivity up to D~2-3, but this value was inside the error bars of both space crafts.

→ The conclusion was done that the emitting electrons mostly have the isotropic pitch-angle distribution.
The isotropization can be done by scattering on plasma waves, whistlers, or magnetic inhomogeneities. (Gordon Emslie mentioned yesterday such a possiblity)

2016 6

HEND (Mars-Odyssey 2001) : stereo effects

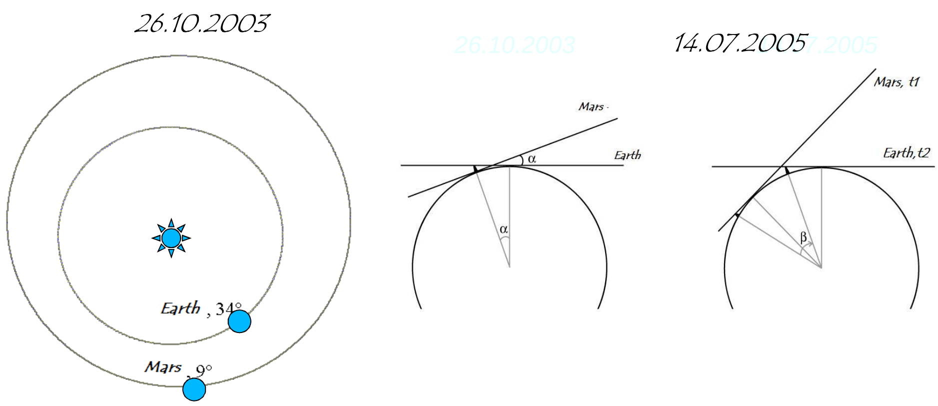

On **14 July 2005**, AR NOAA 10786 was at the west limb for the observations from the Earth. Mars-Odyssey was **39 degrees** to the west from Earth. Thus, flares in this AR were observed as “on disk” flares

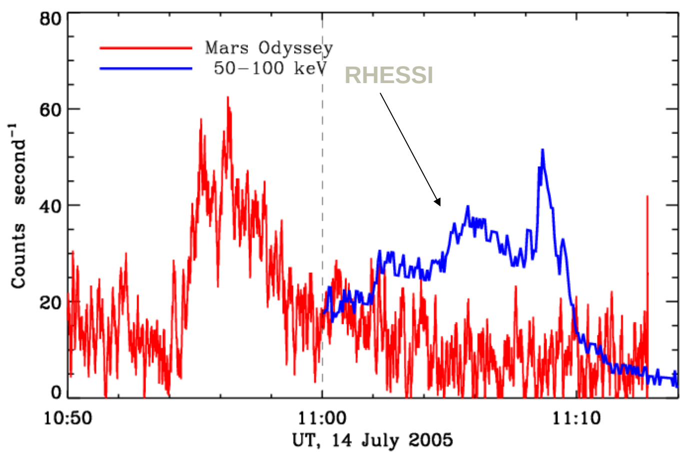

On the late phase of the flare the RHESSI intensity was 2 to 3 times higher than that of HEND. (Livshits et al, 2011)

Polarization degree of hard X-ray emission from solar flares

One more way to get information about the pith-angle distribution of electrons emitting HXR/gamma-ray emissions is to study their polarization.

Measurements of the HXR polarization degree were first carried out more than 40 years ago, but systematic data on a large number of flares are still lacking.

The latest results of measurements carried out by the Coronas-F satellites showed that the degree of HXR polarization in the most energetic flares in 2001–2005 varied from 8 to 40% at the 3σ level at energies lower than 100 keV (Zhitnik et al., 2006).

The results of RHESSI measurements at energies from 100 to 350 keV for six X-class flares yielded a value of 2–54% (Suarez-Garcia et al., 2006).

All the mentioned studies of the HXR directivity and polarization used the integrated emission flux from a whole flare.

Theoretical simulations also did not take into account possible spatial differences of electron distributions in different parts of flaring loop.

Purpose of the current work is to do:

- Simulations of spatial distributions of HXR and gamma-ray emission characteristics on the base of spatial distributions of energetic electrons along a flaring loop obtained via the solution of non-stationary Fokker-Planck equation;
- Comparative analysis of the HXR/Gamma-ray directivity and polarization from different parts of a flaring loop for the cases of isotropic and longitudinal injection of non-thermal electrons to get some observable signatures of the electron pitch-angle anisotropy.

Kinetics of Nonthermal Electrons in Magnetic Loops

In a magnetic loop, a part of injected electrons are trapped due to magnetic mirroring and the other part directly precipitates into the loss-cone. The trapped electrons are scattered due to Coulomb collisions and loose their energy and precipitate into the loss-cone.

A real distribution strongly depends on the injection position in the loop and on the pitch-angle dependence of the injection function *S(E,μ,s,t), and also on time (Melnikov et al. 2006; Gorbikov and Melnikov 2007; Reznikova et al 2009).*

Non-stationary Fokker-Plank equation (Lu and Petrosian 1988):

$$\frac{\partial f}{\partial t} = -c\beta\mu\frac{\partial f}{\partial s} + c\beta\frac{d\ln B}{ds}\frac{\partial}{\partial\mu}\left[\frac{1-\mu^2}{2}f\right] + \frac{c}{\lambda_0}\frac{\partial}{\partial E}\left(\frac{f}{\beta}\right) +$$

$$+\frac{c}{\lambda_0\beta^3\gamma^2}\frac{\partial}{\partial\mu}\left[(1-\mu^2)\frac{\partial f}{\partial\mu}\right] + S(E,\mu,s,t)$$

2016 11

Initial and boundary conditions

Initial condition $f(E,\mu,s,0)=0.$ (no electrons at moment t = 0)

Boundary condition, *s* $f(E,\mu>0,s_{\min},t)=0,\quad f(E,\mu<0,s_{\max},t)=0.$

(precipitated electrons do not come back into the magnetic loop)

Injection function: $S(E,\mu,s,t) = S_1(E)S_2(\mu)S_3(s)S_4(t),$

$S_1(E) = K(E/E_0)^{-\delta}$

$S_2(\mu) = \exp[-(\mu-\mu_1)^2/\mu_0^2]$ μ_0= 0.2, μ_1= 1

$S_3(s) = \exp[-(s-s_1)^2/s_0^2]$ s_1=0 cm, s_0= 2 10^8 cm

$S_4(t) = \exp[-(t-t_1)^2/t_0^2]$ t_1=25 s, t_0=14 s

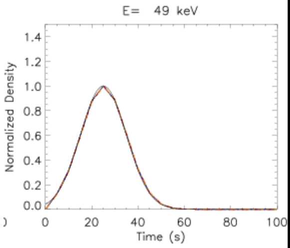

Normalization:

$\int S(E,\mu,s,t)\, dE\, d\mu\, ds\, dt = N_{tot}$

12

Parameters of the model loop

Magnetic field distribution:

$$B(s) = B_0 \exp[(s-s_1)^2/ s_2^2],$$

where $s_2^2 = s^2_{max}/\ln(B_c/B_0)$, B_0 and B_c *are the magnetic inductions in the center and footpoints of the loop*, $s_1 = 0$, $s_{max} = 3\ 10^9 cm$ are coordinates of the loop center and footpoints, $k = B_c/B_0$ mirror ratio, k=2; k=5

Electron number density distribution in the coronal part of the loop:

$$n(h)=n_0 \exp((R-h)/h_c)$$

where $h_c = 1.3\ 10^9 cm$, $n_0 = 5\ 10^{10}\ cm^{-3}$.

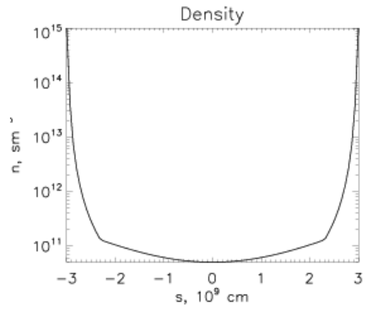

In the chromosphere [Aschwanden et al, 2002]:

$$n(h)=10^{12}(h/h_{ch})^{-2.5}$$

where $h_{ch} = 3\ 10^8$ cm – height scale of the chromosphere

2016 13

Injection Models

Case 1:
Isotropic Injection at the Loop Top

$$S_2(\mu) = 1$$

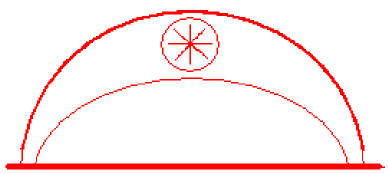

Case 2:
Anisotropic Injection at the Loop Top in the right-hand direction

$$S_2(\mu) = exp[-(\mu - 1)^2/\mu_0^2]$$

mu_0=0.2, ($\Delta\alpha$ =36^o)

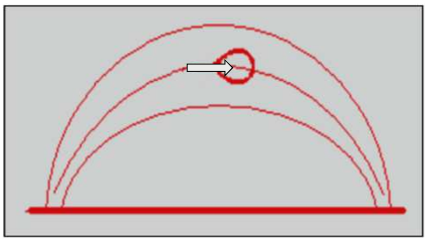

2014 14

Case 1: Isotropic Injection at the Loop Top

Normalized distribution function of energetic electrons over pitch-angles

Looptop | Footpoint

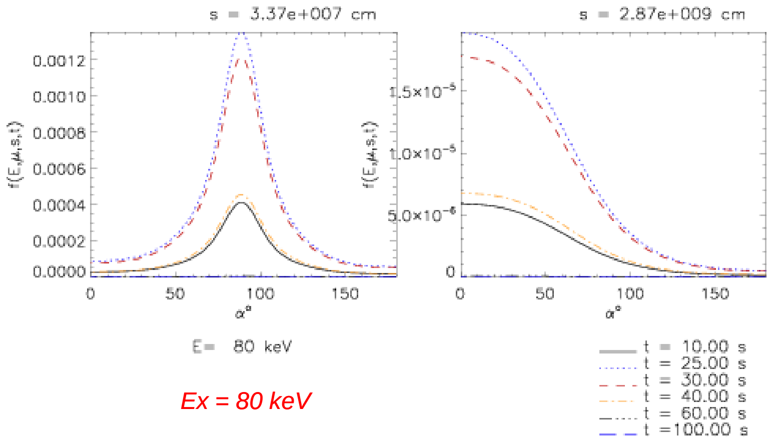

Ex = 80 keV

2016

Case 1: Isotropic Injection at the Loop Top

Normalized distribution function of energetic electrons over pitch-angles

Looptop | Footpoint

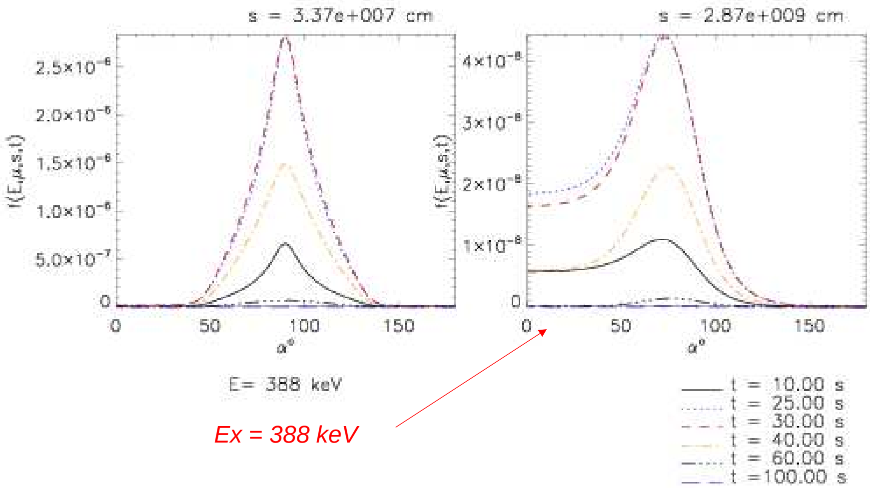

Ex = 388 keV

Case 2: Anisotropic Injection at the Loop Top

Normalized distribution function of energetic electrons over pitch-angles

Ex = 49 keV

Ex = 388 keV

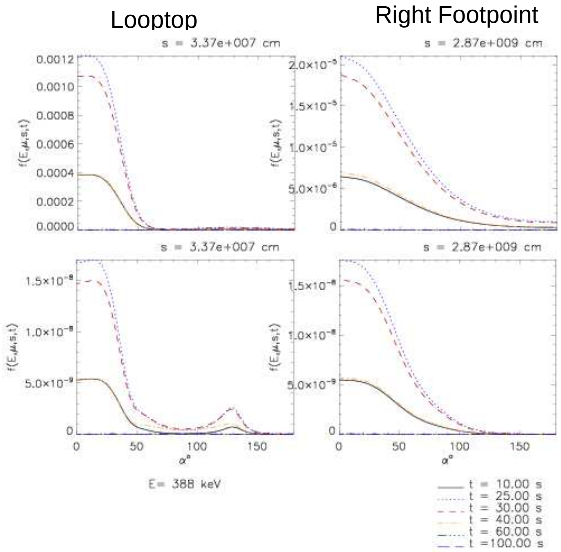

2016 17

Distribution of HXR-emission along the Loop

Differential HXR intensity (per unit length):

$$\frac{dI(\varepsilon,\alpha,s,t\_)}{ds}=\frac{S(s)\times n(s)}{R^2}\int_{\varepsilon}^{\infty}\mathrm{v(E)\,dE}\int_{-1}^{1} f(E,s,\mu,t)d\mu\int_{0}^{2\pi}\sigma(\varepsilon,E,\alpha,\mu,\varphi)d\varphi$$

where $S(s)$ is the area of the transverse crosssection of the source (loop) in the general case and depends on the coordinate along the axis of the magnetic loop (decreases with an increase in s); $n(s)$ is the concentration of plasma ions (depends on coordinate s and is determined using a model); and $R = 1.5 \times 10^{13}$ cm is the astronomical unit. The dependence of the area of the transverse cross-section on coordinate s is determined from the condition of the invariance of the magnetic flux $B(s)S(s)$ = const and model dependence of the magnetic field on coordinate s.

The total (summated over the polarization) relativistic cross-section of bremsstrahlung radiation σ was obtained in (Gluckstern and Hull, 1953).

Directivity of X-ray and gamma-ray emission
Case 1: isotropic injection at the loop top, hard spectrum: delta=3

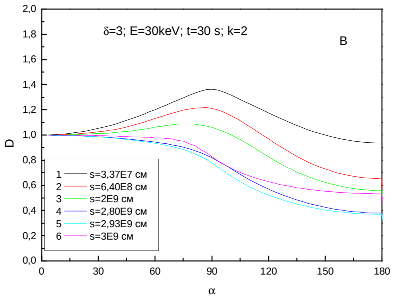

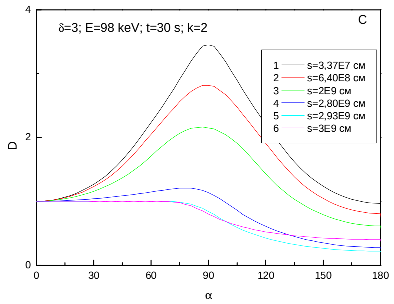

Directivity of HXR and gamma-rays:

D(α,ε,s,t)=I(α,ε,s,t)/I(α=0, ε,s,t)

α= angle(**k B**);
ε – photon energy,
s – position along the loop;
t – time

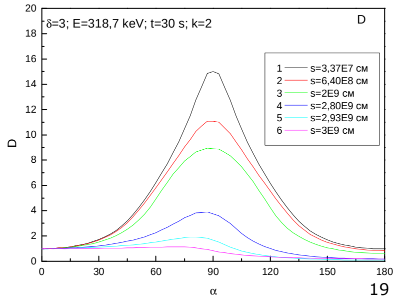

2016 19

Directivity of X-ray and gamma-ray emission
Case 2: longitudinal injection at the loop top, hard spectrum: delta=3

Left half of loop

Right half of loop

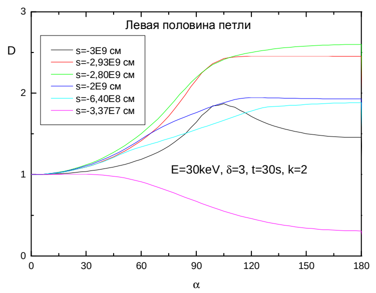

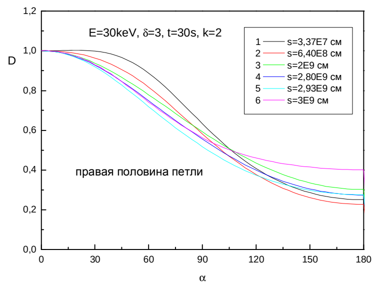

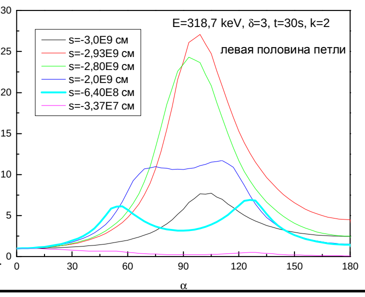

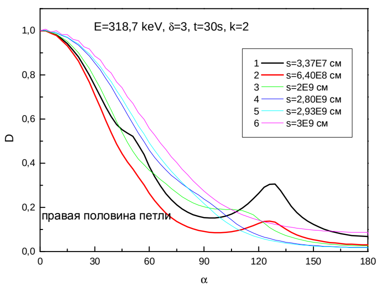

2014 20

Angular characteristics of polarization degree of hard X-ray emission from different parts of flaring magnetic loops

The degree of HXR polarization is defined by the difference between intensities in the **kB** plane (I_1) and perpendicular to it (I_2) as follows:

$$P = (I_2 - I_1)/(I_2 + I_1)$$

The I_2 and I_1 intensities are determined via the corresponding cross-sections of the σ_1 and σ_2 bremsstrahlung mechanism (Gluckstern and Hull, 1953).

Angular characteristics of polarization degree of hard X-ray emission from different parts of flaring magnetic loops

Case 1: isotropic injection *Case 2: longitudinal injection*

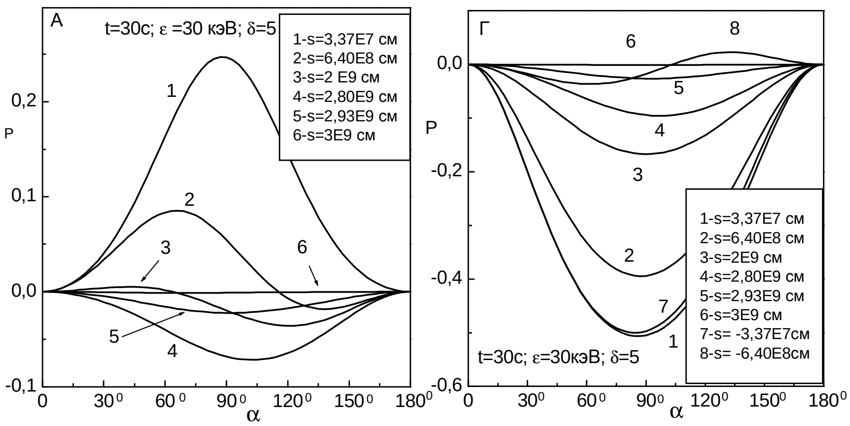

Degree of linear polarization of HXR in the case of isotropic (left hand panel) and anisotropic (right hand panel) injections.

2016 22

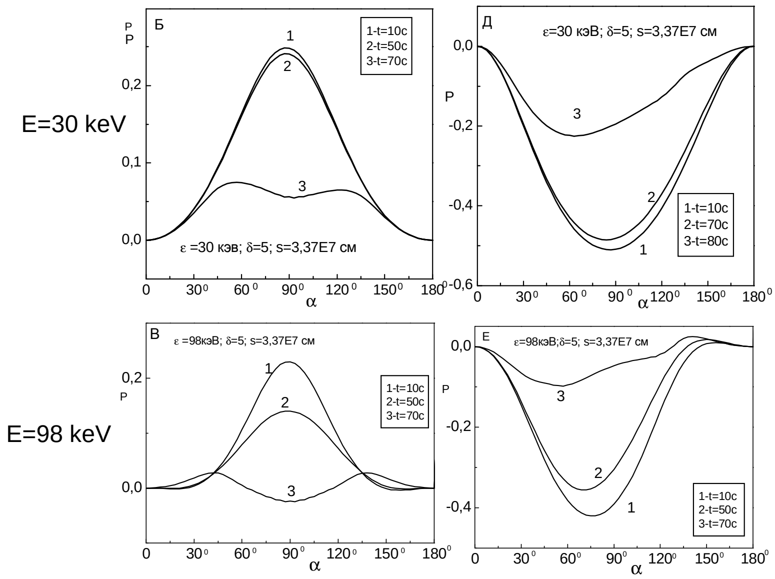

Dynamics of linear polarization of HXR at E=30 keV and E=98 keV in the case of isotropic (left hand panel) and anisotropic (left hand panel) injections.

Conclusions

The degree of directivity and polarization and the variation of these parameters in time depend on the position within the loop and vary fundamentally between cases of isotropic and anisotropic (longitudinal) injection of electrons.

The revealed properties of the directivity and polarization dynamics may be used in X-ray and gamma ray diagnostics of the type of pitch-angle distribution of electrons accelerated in a certain specific observed flare.

As a consequence, spatially resolved hard X-ray observations may provide us with new constraints on particle acceleration mechanisms and models.

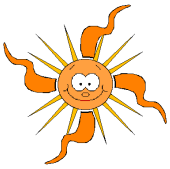

Thank you for your attention!